PSFC/JA-03-12

# Drift Ballooning Instabilities in Tokamak Edge Plasmas

R.J. Hastie, J.J. Ramos, and F. Porcelli

June, 2003.

Plasma Science and Fusion Center
Massachusetts Institute of Technology
Cambridge MA 02139, U.S.A.

This work was supported by the U.S. Department of Energy under Grant No. DE-FG02-91ER-54109.

# Drift Ballooning Instabilities in Tokamak Edge Plasmas

R.J. Hastie[1,2], J.J. Ramos[1] and F. Porcelli[3]

[1]Plasma Science and Fusion Center, Massachusetts Institute of Technology, Cambridge MA, U.S.A.

[2]EURATOM/UKAEA Fusion Association, Culham Science Centre, Abingdon, U.K.

[3]Instituto Nazionale Fisica della Materia, Politecnico di Torino, Italy

## Abstract

The linear stability of high-toroidal-number drift-ballooning modes in tokamaks is investigated with a model that includes resistive and viscous dissipation, and assumes the mode frequency to be comparable to both the sound and diamagnetic frequencies. The coupled effect of ion drift waves and electron drift-acoustic waves is shown to be important, resulting in destabilization over an intermediate range of toroidal mode numbers. The plasma parameters where the assumed orderings hold would be applicable to the edge conditions in present day tokamaks, so these instabilities might be related to the observed quasi-coherent edge-localized fluctuations.

## 1. Introduction.

Recent observations [1] of a localized instability (the quasi-coherent mode) in the edge pedestal of some H-mode discharges in the Alcator C-Mod tokamak appear to be inconsistent with linear stability predictions for ideal ballooning modes, because the local pressure gradient in the pedestal may be insufficient to drive the ideal-magnetohydrodynamic (MHD) instability. Resistive drift ballooning modes might, however, explain the observations. Several recent studies, both linear [2,3,4] and non-linear [4,5,6], have been devoted to this topic. In much of this work, a complex set of two-fluid Braginskii [7] equations is solved numerically, sometimes in a complicated equilibrium containing or simulating the proximity of a magnetic separatrix and scrape-off layer. Instability is generally found, but there has been little discussion of a stability threshold. However, the experimental observations on Alcator indicate that there is a stability threshold which separates "edge-localized-mode (ELM) free" H-mode behavior, in which the edge plasma is fluctuation free, from "enhanced $D_\alpha$" (EDA) behavior, in which the quasi-coherent mode is present in the edge pedestal. In addition, at higher levels of auxilliary heating power, the quasi-coherent mode is replaced by a broad spectrum of grassy ELMs [8]. It is possible that these observations may be explained by a linear stability threshold, with initially a single mode (one toroidal mode number $n_\varphi$) becoming unstable, followed by an increasing spectrum of unstable $n_\varphi$ values. Although ideal-MHD ballooning modes might be near their stability threshold, electron and ion diamagnetic corrections are likely to be important, as are interactions with acoustic waves. Dissipative effects (especially resistive effects) are also likely to be important.

In this paper we investigate the linear stability of drift ballooning modes using a simple model for the plasma equilibrium (the $s-\alpha$ model [9]), but including a variety of non-ideal physical effects. We derive a simple eigenmode equation for drift ballooning modes by considering an optimal ordering in which $\omega \sim \omega_s \sim \omega_{*j} \sim \mu k_\perp^2 \sim \eta_\parallel k_\perp^2 \sim \eta_\perp k_\perp^2$, where $\omega$ is the mode frequency, $\omega_s = c_s/Rq$ is the frequency for sound propagation over a connection length, with $c_s^2 = (T_i + T_e)/m_i$, $q$ the safety factor and $R$ the major toroidal radius, $\omega_{*j} = (\mathbf{k}\times\mathbf{B})\cdot\nabla p_j/(neB^2)$ is the diamagnetic frequency for species $j$, $\mu = 0.3\nu_{ii}\rho_i^2$ is the classical perpendicular viscosity with $\rho_i = [T_i m_i/(e^2B^2)]^{1/2}$ the ion Larmor radius, and $\eta_\parallel$ and $\eta_\perp$ are the longitudinal and transverse Spitzer resistivities. The $s-\alpha$ equilibrium

model with $s = rq'/q$ and $\alpha = -2Rp'q^2/B^2 \sim O(1)$ is employed and a two length scale averaging formalism is developed, using $\omega/\omega_A \ll 1$ as the expansion parameter, where $\omega_A$ is the Alfven frequency, $\omega_A = c_A/Rq$ with $c_A^2 = B^2/(nm_i)$. The resulting eigenvalue equation contains the following physical effects: (1)Ideal-MHD instability drive (through the boundary condition). (2) Resistive diffusion leading to resistive ballooning modes. (3) Sound wave propagation. (4) Two-fluid diamagnetic effects which modify sound waves into electron drift-acoustic modes and introduce ion finite-Larmor-radius (FLR) effects. (5) Perpendicular ion viscosity. The two different classes of resistive ballooning modes, namely those driven locally in radius by the geodesic curvature (the Carreras-Diamond modes [10]) and those driven by the ideal-MHD energy (characterized by the stability index $\Delta'_B$ [11-13]) are both described by the eigenmode equation.

In Section 2 the linear theory of dissipative drift ballooning modes is developed from a set of linearized two-fluid equations [14,15]. These fluid equations are appropriate for the short mean-free path conditions of the edge plasma in Alcator C-Mod. They describe isothermal ions and electrons in a strong magnetic field toroidal equilibrium without temperature gradients. This linearized system contains four first order ballooning equations: continuity, parallel momentum, Ohm's law and vorticity. Eliminating the parallel ion flow, $\tilde{v}_{\|i}$, and the parallel component of the perturbed magnetic vector potential, $\tilde{A}_\|$, generates a pair of coupled second order ODEs, describing shear-Alfven and sound waves. This system is then specialized to the $s - \alpha$ equilibrium model. In Section 3 a perturbative solution of the 4th order ballooning system is developed by means of a two-scale analysis. This yields a 2nd order resistive layer equation on the long scale of the ballooning variable $s\theta \gg 1$. The relevant dispersion relations are obtained by matching the resistive layer solution to the solution in the ideal-MHD region $s\theta \sim 1$. In Section 4 the stability of FLR-modified ideal-MHD modes is discussed. This differs from previous analyses [16,17] by including the coupling to electron drift-acoustic modes. The main consequence is that the FLR stabilisation of ideal ballooning modes is completely suppressed at intermediate values of toroidal mode number $n_\varphi$. In Section 5 the stability of drift resistive ballooning modes is discussed and in Section 6 the effects of perpendicular ion viscosity are outlined. Finally, a summary and overview of drift ballooning stability is presented in Section 7.

## 2. Two-Fluid Equations for Dissipative Drift Ballooning Modes.

In this section, starting from a set of linearized two-fluid equations for isothermal ions and electrons and using the $s-\alpha$ equilibrium model to describe the edge pedestal region of a tokamak, we derive the appropriate eigenmode equations for drift ballooning modes whose frequencies and growth rates are sub-Alfvenic. A simple reduced set of two-fluid equations has been given in Refs. [14,15]. Taking the linearized version of Eqs.(31-36) of [15] with $\omega = i\partial/\partial t$, and further simplifying these equations by assuming that the equilibrium ion and electron temperatures are constant and equal, and ions and electrons are isothermal, the following system of ballooning equations is obtained for the four dimensionless perturbed fields $\hat{n} = \tilde{n}/n$, $\hat{\phi} = e\tilde{\phi}/T_e$, $\hat{v}_\parallel = \tilde{v}_{\parallel i}/c_s$ and $\hat{\psi} = e\tilde{A}_\parallel c_s/T_e$, where $\tilde{n}$, $\tilde{v}_{\parallel i}$, $\tilde{\phi}$ and $\tilde{A}_\parallel$ are the perturbed density, parallel ion flow, electrostatic potential and parallel component of the vector potential, respectively:

$$\omega\hat{n} - \omega_{*e}\hat{\phi} \;=\; (2\omega_\kappa - \omega k_\perp^2\rho_i^2)(\hat{\phi}+\hat{n}) \;+\; c_s k_\parallel \hat{v}_\parallel \;-\; i\eta_\perp k_\perp^2 \frac{c_s^2}{c_A^2}\hat{n}, \tag{1}$$

$$\omega\hat{v}_\parallel + \omega_{*e}\hat{\psi} \;=\; c_s k_\parallel \hat{n} \;-\; 4i\mu k_\perp^2 \hat{v}_\parallel, \tag{2}$$

$$(\omega - \omega_{*e})\hat{\psi} \;=\; c_s k_\parallel (\hat{\phi} - \hat{n}) \;-\; i\eta_\parallel k_\perp^2 \hat{\psi}, \tag{3}$$

$$\omega k_\perp^2\rho_i^2(\hat{\phi}+\hat{n}) \;=\; 4\omega_\kappa \hat{n} \;+\; \frac{c_A^2}{c_s} k_\parallel (k_\perp^2\rho_i^2\hat{\psi}) \;-\; i\mu k_\perp^4\rho_i^2(\hat{\phi}+\hat{n}). \tag{4}$$

Here we have introduced $\omega_\kappa = p_i(\mathbf{k}\times\mathbf{B})\cdot\kappa/(neB^2)$, $\kappa = [(\mathbf{B}/B)\cdot\nabla](\mathbf{B}/B)$ being the magnetic curvature. The perpendicular viscous stress terms and the transverse particle diffusion ($\propto \eta_\perp$) in these equations do not appear in Ref.[15], and these terms were taken from Ref.[14]. Equation(1) is the ion continuity equation, Eq.(2) the parallel momentum equation, Eq.(3) the generalized Ohm's law and Eq.(4) is the vorticity equation. These equations are to be considered valid in leading order of the short-perpendicular-wavelength ballooning expansion, $k_\parallel/k_\perp \sim r/(n_\varphi q^2 R) \ll 1$, for the ballooning representation variables. Therefore, $k_\parallel = -i\nabla_\parallel$ is a differential operator but $k_\perp$ is just a function of the spatial variables. Eliminating $\hat{v}_\parallel$ and $\hat{\psi}$ from these equations, we arrive at a pair of second order ODE ballooning equations for the new dependent variables

$$U = \hat{\phi} - \hat{n}, \tag{5}$$

and

$$V = \frac{\omega}{\omega_{*e}}\hat{n} - \hat{\phi}, \tag{6}$$

describing the coupling of shear-Alfven waves and drift-acoustic waves.

Next we specialize the ballooning equations to the $s-\alpha$, large-aspect-ratio, circular tokamak equilibrium model [9]. In this equilibrium, the parallel gradient operator becomes $ic_s k_\parallel = \omega_s\, d/d\theta$, where $\theta$ is the ballooning extended poloidal variable, $-\infty < \theta < \infty$. The perpendicular wavenumber is $k_\perp = (n_\varphi q/r)\hat{k}_\perp(\theta)$, with $\hat{k}_\perp^2(\theta) = 1+(s\theta-\alpha\, sin\theta)^2$. The ratio between the curvature and diamagnetic frequencies is $\omega_\kappa/\omega_{*i} = [2\omega_s^2 q^2/(\omega_A^2\alpha)]g(\theta)$ with $g(\theta) = cos\theta + (s\theta - \alpha\, sin\theta)sin\theta$, and the ion Larmor radius is related to the diamagnetic frequency and MHD variables through $\rho_i^2 = 8[\omega_s\omega_{*i}r/(\omega_A^2 n_\varphi\alpha)]^2$. We also define the resistive and viscous frequencies $\omega_\eta \equiv \eta_\parallel(n_\varphi q/r)^2$ and $\omega_\mu \equiv \mu(n_\varphi q/r)^2$. Then the shear-Alfven equation takes the form:

$$\begin{aligned}\frac{d}{d\theta}\left[\frac{(\omega-\omega_{*e})\hat{k}_\perp^2}{\omega-\omega_{*e}+i\omega_\eta\hat{k}_\perp^2}\,\frac{dU}{d\theta}\right] + \frac{(\omega-\omega_{*i})(\omega+i\omega_\mu\hat{k}_\perp^2)}{\omega_A^2}\,\hat{k}_\perp^2\, U = \\ = -\alpha\, g\,(U+V) + \frac{2\omega_{*i}(\omega+i\omega_\mu\hat{k}_\perp^2)}{\omega_A^2}\,\hat{k}_\perp^2\, V,\end{aligned} \tag{7}$$

and the drift-acoustic equation takes the form:

$$\begin{aligned}\frac{d^2V}{d\theta^2} + \frac{(\omega-\omega_{*e})(\omega+4i\omega_\mu\hat{k}_\perp^2)}{\omega_s^2}\,V = \\ = \left[-4q^2(\omega+4i\omega_\mu\hat{k}_\perp^2)\left(\frac{g}{\omega_A^2\alpha}+\frac{2\omega\omega_{*e}\hat{k}_\perp^2}{\omega_A^4\alpha^2}\right)+\frac{i\omega_\eta\hat{k}_\perp^2(\omega+i\omega_\mu\hat{k}_\perp^2)}{\omega_A^2(\omega-\omega_{*e})}\right]\left[(\omega-\omega_{*i})U-2\omega_{*i}V\right] + \\ + \left[\frac{i\omega_\eta\alpha g}{\omega-\omega_{*e}} - \frac{\eta_\perp}{\eta_\parallel}\,\frac{i\omega_\eta\hat{k}_\perp^2(\omega+4i\omega_\mu\hat{k}_\perp^2)}{\omega_A^2}\right](U+V) + \\ + \frac{d}{d\theta}\Big[ln(\omega+4i\omega_\mu\hat{k}_\perp^2)\Big]\left[\frac{i\omega_\eta\hat{k}_\perp^2}{\omega-\omega_{*e}+i\omega_\eta\hat{k}_\perp^2}\,\frac{dU}{d\theta}+\frac{dV}{d\theta}\right].\end{aligned} \tag{8}$$

By setting $\mu \to 0$, $\omega_{*j}/\omega \to 0$ and $\eta_\perp \to \eta_\parallel$ these equations reduce to the isothermal single fluid resistive MHD equations [18].

## 3. Two-Scale Averaging of the Drift Ballooning Equations.

Under plasma conditions of interest for magnetic fusion, including tokamak edge conditions, the characteristic resistive diffusion time $\tau_\eta$ is orders of magnitude longer than the characteristic Alfven time $\tau_A = 1/\omega_A$. Therefore we can introduce the natural dimensionless resistivity parameter

$$\epsilon_\eta \equiv \left(\frac{\omega_\eta}{\omega_A}\right)^{1/3} = \left(\frac{\eta_\parallel n_\varphi^2 q^2}{r^2 \omega_A}\right)^{1/3} = \left(n_\varphi q\right)^{2/3} \left(\frac{\tau_A}{\tau_\eta}\right)^{1/3} \ll 1, \tag{9}$$

and use it as the basic small expansion parameter for a perturbative solution of our drift ballooning equations. The growth rates of resistive modes typically fall within the "drift ordering", being comparable to the diamagnetic drift frequency but much less than the Alfven frequency, $\gamma \sim \omega_{*j} \ll \omega_A$. In order to also take into account the sound wave effects, we will carry out our perturbative solution assuming the maximal orderings:

$$\omega \sim \omega_s \sim \omega_{*j} \sim \epsilon_\eta \, \omega_A. \tag{10}$$

Besides, we assume that the viscosity is smaller than or comparable to the resistivity:

$$\omega_\mu \lesssim \omega_\eta \equiv \epsilon_\eta^3 \, \omega_A. \tag{11}$$

Accordingly, we define the normalized dimensionless frequencies $\hat{\omega} \equiv \omega/(\epsilon_\eta \, \omega_A)$, $\hat{\omega}_s \equiv \omega_s/(\epsilon_\eta \, \omega_A)$ and $\hat{\omega}_{*j} \equiv \omega_{*j}/(\epsilon_\eta \, \omega_A)$, as well as $\hat{\mu} \equiv \omega_\mu/\omega_\eta = \mu/\eta_\parallel$. It follows that the resistivity, the viscosity and the inertia only become important at large values of the ballooning variable: $s\theta \sim \epsilon_\eta^{-1} \gg 1$. In this domain, to be termed the resistive layer, all the frequencies, $\omega$, $\omega_s$, $\omega_{*j}$, $\eta_\parallel k_\perp^2 \simeq \omega_\eta (s\theta)^2$ and $\mu k_\perp^2 \simeq \omega_\mu (s\theta)^2$, are comparable and of the order of $\epsilon_\eta \, \omega_A$.

For $s\theta \sim 1$ hence $\hat{k}_\perp^2(\theta) \sim 1$, a domain to be called the ideal-MHD region, the effects of the resistivity, the viscosity and the inertia are negligible. Here, to zeroth order in $\epsilon_\eta$, the drift-acoustic equation is simply

$$\frac{d^2 V_0(\theta)}{d\theta^2} + \frac{\omega(\omega - \omega_{*e})}{\omega_s^2} \, V_0(\theta) = 0, \tag{12}$$

whose only solution that can be continued through the resistive layer in such a way that it vanishes at infinity is $V_0(\theta) = 0$. Then, also to zeroth order in $\epsilon_\eta$, the shear-Alfven equation reduces to

$$\frac{d}{d\theta}\left[\hat{k}_\perp^2(\theta) \, \frac{dU_0(\theta)}{d\theta}\right] + \alpha \, g(\theta) \, U_0(\theta) = 0, \tag{13}$$

whose solution is $U_0(\theta) = U_{ideal}(\theta; \omega^2 = 0)$, the ideal-MHD solution in the absence of inertia. Its asymptotic behavior at large $|\theta|$ is

$$U_0(|\theta| \to \infty) = U_{ideal}(|\theta| \to \infty; \omega^2 = 0) = \frac{1}{\Delta'_B} + \frac{1}{s|\theta|} \tag{14}$$

for an even parity mode or

$$U_0(|\theta| \to \infty) = U_{ideal}(|\theta| \to \infty; \omega^2 = 0) = \frac{sign(\theta)}{\Delta'_B} + \frac{1}{s\theta} \tag{15}$$

for an odd parity mode. The constant $1/\Delta'_B$ is proportional to the incremental ideal-MHD potential energy, $\delta W$, associated with the ballooning perturbation so that positive, zero and negative values of $1/\Delta'_B$ correspond to ideal-MHD stability, marginality and instability respectively.

In the resistive layer, i.e. $s\theta \sim \epsilon_\eta^{-1} \gg 1$, we carry out a two-scale perturbation analysis, introducing the slow variable $Z = \epsilon_\eta s\theta$ in the secular terms of the ballooning equations and reserving the $\theta$ notation for the fast variable in the periodic terms. Thus we write:

$$\frac{d}{d\theta} \to \frac{\partial}{\partial\theta} + \epsilon_\eta s \frac{\partial}{\partial Z}, \tag{16}$$

$$\hat{k}_\perp^2(\theta) \to 1 + (Z/\epsilon_\eta - \alpha\ sin\theta)^2, \tag{17}$$

$$g(\theta) \to cos\theta + sin\theta(Z/\epsilon_\eta - \alpha\ sin\theta), \tag{18}$$

and expand the linearized ballooning equations with

$$U(\theta, Z) = U_0(\theta, Z) + \epsilon_\eta\ U_1(\theta, Z) + \epsilon_\eta^2\ U_2(\theta, Z) + \dots\ , \tag{19}$$

$$V(\theta, Z) = \epsilon_\eta\ V_1(\theta, Z) + \epsilon_\eta^2\ V_2(\theta, Z) + \dots\ . \tag{20}$$

With this ordering, the shear-Alfven equation yields in zeroth order:

$$\frac{\partial}{\partial\theta}\left[\frac{Z^2}{1 + iZ^2/(\hat{\omega} - \hat{\omega}_{*e})}\ \frac{\partial U_0}{\partial\theta}\right] = 0, \tag{21}$$

whose solution is $U_0 = U_0(Z)$. In first order we solve for $U_1(\theta, Z)$ and $V_1(\theta, Z)$ to obtain

$$U_1(\theta, Z) = \frac{\alpha\ sin\theta}{Z}\left(1 + \frac{iZ^2}{\hat{\omega} - \hat{\omega}_{*e}}\right) U_0(Z), \tag{22}$$

$$V_1(\theta, Z) \;=\; Z\; sin\theta\; \frac{4q^2(\hat{\omega}-\hat{\omega}_{*i})(\hat{\omega}+4i\hat{\mu}Z^2)/\alpha \;+\; i\alpha/(\hat{\omega}-\hat{\omega}_{*e})}{1 \;-\; (\hat{\omega}-\hat{\omega}_{*e})(\hat{\omega}+4i\hat{\mu}Z^2)/\hat{\omega}_s^2}\; U_0(Z). \tag{23}$$

In second order a pair of equations for $U_2(\theta, Z)$ and $V_2(\theta, Z)$ is obtained. The condition for solubility of the equation for $U_2(\theta, Z)$ in the fast scale variable, yields the following secular equation that determines the leading order eigenfunction $U_0(Z)$:

$$s^2\; \frac{d}{dZ}\left[\frac{Z^2}{1+iZ^2/(\hat{\omega}-\hat{\omega}_{*e})}\frac{dU_0}{dZ}\right] \;+\; (\hat{\omega}-\hat{\omega}_{*i})(\hat{\omega}+i\hat{\mu}Z^2)Z^2\; U_0 \;+ \tag{24}$$

$$+\; \alpha\; Z\; <sin\theta(U_1+V_1)>_\theta \;-\; \frac{\alpha^2}{2}\; U_0 \;=\; 0,$$

where $< ... >_\theta$ indicates the average over the fast, periodic variable $\theta$. This equation is subject to the boundary conditions,

$$U_0(Z \to \infty) = 0 \tag{25}$$

as required by the ballooning representation, and

$$U_0(Z \to 0) = \frac{1}{\Delta'_B} + \frac{\epsilon_\eta}{Z}, \tag{26}$$

to match the solution (14) or (15) in the ideal-MHD region. The solution of this boundary problem yields the sought after dispersion relation for our dissipative drift ballooning modes. Transforming to a newly normalized secular variable $X^2 = iZ^2/(\hat{\omega}-\hat{\omega}_{*e})$, the resistive layer eigenmode equation can be cast in the form:

$$s^2\; \frac{d}{dX}\left(\frac{X^2}{1+X^2}\frac{dU_0}{dX}\right) \;-\; \left[X^2Q(X^2) \;+\; X^4T(X^2)\right]\; U_0 \;=\; 0, \tag{27}$$

where

$$Q(X^2) \;=\; i\hat{\omega}(\hat{\omega}-\hat{\omega}_{*i})(\hat{\omega}-\hat{\omega}_{*e})\left[1+2q^2P(X^2)\right] \;-\; \frac{\alpha^2}{2}\left[1-P(X^2)\right], \tag{28}$$

$$T(X^2) \;=\; i\hat{\mu}(\hat{\omega}-\hat{\omega}_{*i})(\hat{\omega}-\hat{\omega}_{*e})^2\left[1+8q^2P(X^2)\right], \tag{29}$$

and

$$P(X^2) \;=\; \frac{\hat{\omega}_s^2}{\hat{\omega}_s^2 \;-\; (\hat{\omega}-\hat{\omega}_{*e})\left[\hat{\omega}+4\hat{\mu}(\hat{\omega}-\hat{\omega}_{*e})X^2\right]}. \tag{30}$$

Equation 24 (or equivalently 27) describes the coupling of visco-resistive ballooning modes to drift-acoustic waves. The novel feature of the foregoing two-scale analysis lies in the ordering $\omega/\omega_s \sim 1$. In much previous analyses, either $\omega/\omega_s \ll 1$ or $\omega/\omega_s \gg 1$ was assumed. As a result of the $\omega/\omega_s \ll 1$

ordering, $V_0(Z) \neq 0$ and a 4th order coupled set of averaged equations is obtained [12,19]. In this limit, the geodesic curvature drive for the Carreras-Diamond resistive ballooning mode (the term proportional to $\alpha^2$ in the expression for $Q$) is lost and only resistive ballooning modes which are driven by $\Delta'_B$ are found. With $\omega/\omega_s \gg 1$, sound wave propagation is neglected and the resistive ballooning modes of the Carreras-Diamond type are found [10,12,20,21,22]. Our equations provide a bridge between these two extremes, not only for studying resistive ballooning modes but also for investigating finite-Larmor-radius effects on ideal ballooning modes [16,17]. These problems will be revisited in the next sections.

## 4. Effect of Drift-Acoustic Waves on FLR Stabilization of Ideal Ballooning Modes.

The above two-scale formalism can be used to study diamagnetic drift and drift-acoustic effects on ideal modes. For this purpose, we will consider in this section an ideal-MHD unstable equilibrium, i.e. $\Delta'_B < 0$, where resistive and viscous dissipation are negligible. Then, in the limit $\eta \to 0$, $\mu \to 0$ Eq.(24) becomes

$$s^2 \frac{d}{dZ}\left(Z^2 \frac{dU_0}{dZ}\right) + (1+2q^2P_0)\,\omega\,(\omega-\omega_{*i})\,\frac{Z^2}{\omega_A^2\epsilon_\eta^2}\,U_0 = 0, \tag{31}$$

where

$$P_0 \equiv P(\mu=0) = \frac{\omega_s^2}{\omega_s^2 - \omega(\omega-\omega_{*e})}. \tag{32}$$

Its solution decaying at infinity is

$$U_0(Z) = \frac{\epsilon_\eta}{Z}\, exp\left(-\left[-(1+2q^2P_0)\omega(\omega-\omega_{*i})\right]^{1/2}\frac{Z}{s\omega_A\epsilon_\eta}\right), \tag{33}$$

and imposing the matching condition (26) as $Z \to 0$ we obtain the dispersion relation for compressible, dissipation-free ballooning modes in the presence of diamagnetic drift effects:

$$-\frac{s\omega_A}{\Delta'_B} = \left[-(1+2q^2P_0)\omega(\omega-\omega_{*i})\right]^{1/2}, \tag{34}$$

or

$$-\omega(\omega-\omega_{*i})\left[(1+2q^2)\omega_s^2 - \omega(\omega-\omega_{*e})\right] = \left(\frac{s\omega_A}{\Delta'_B}\right)^2\left[\omega_s^2 - \omega(\omega-\omega_{*e})\right]. \tag{35}$$

The quantity $-1/\Delta'_B$ is a measure of the ideal-MHD energy, $-\delta W$, available to drive the ballooning instability. It is convenient to characterize this energy in terms of the ideal-MHD growth rate

$$\gamma_I = -\frac{s\omega_A}{(1+2q^2)^{1/2}\Delta'_B} \tag{36}$$

which would be obtained in the incompressible limit, $\omega_s/\gamma_I \to \infty$, in the absence of diamagnetic effects. So, the right-hand side of Eq.(35) contains the ideal-MHD instability drive while the left-hand side indicates the presence of three waves: an ion drift wave, $\omega = \omega_{*i}$, and a pair of toroidally modified electron drift-acoustic waves, $\omega(\omega - \omega_{*e}) = (1+2q^2)\omega_s^2$. The effect of the electron drift-acoustic waves is lost in both the $\omega_s \to \infty$ and $\omega_s \to 0$ limits: for $\omega_s/\omega \to \infty$ we have $-\omega(\omega - \omega_{*i}) = \gamma_I^2$, and for $\omega_s/\omega \to 0$ we get $-\omega(\omega - \omega_{*i}) = \gamma_I^2(1+2q^2)$. These standard FLR results are illustrated in Fig.1, where the $\omega_s = \infty$ and $\omega_s = 0$ growth rates are plotted versus the toroidal mode number $n_\varphi$, for the choice of parameters $s = 2$, $q = 5$, $\omega_{*i}/(n_\varphi\omega_A) = -\omega_{*e}/(n_\varphi\omega_A) = 0.02$ and $\Delta'_B = -50$ which corresponds to $\alpha = 1.185 = 1.01\ \alpha_{crit}$. All short wavelength modes with $n_\varphi$ above the critical value such that $|\omega_{*i}|/2$ exceeds $\gamma_I$ in the $\omega_s = \infty$ case, or $\gamma_I(1+2q^2)^{1/2}$ in the $\omega_s = 0$ case, are stabilized.

The standard FLR results are dramatically modified when we consider the complete dispersion relation (35), including the coupling to electron drift-acoustic waves at finite $\omega_s$. Now, instead of the simplified quadratic dispersion relations of the standard FLR treatments, we have a quartic dispersion relation with two more roots associated with the two branches of electron drift-acoustic waves, some of which may yield a new positive growth rate. This is illustrated in Fig.2, where the growth rate is again plotted versus $n_\varphi$ for the same parameters used in Fig.1, but now $\omega_s = 0.05\ \omega_A$. Here, in contrast to Fig.1, both low and high $n_\varphi$ modes are FLR stabilized but an island of instability appears at intermediate $n_\varphi$ values. This occurs in the neighborhood of that $n_\varphi$ at which the ion drift wave is resonant with a branch of the drift acoustic waves:

$$\omega_{*i}(\omega_{*i} - \omega_{*e}) = (1+2q^2)\omega_s^2. \tag{37}$$

At this $n_\varphi$ value, the electron drift-acoustic waves have frequencies $\omega = 2\omega_{*e}$ and $\omega = \omega_{*i}$, and the quartic dispersion relation (35) has two roots close to $\omega_{*i}$, one of which develops a positive growth rate:

$$\omega = \omega_{*i} \pm i\frac{2q}{\sqrt{3}}\gamma_I + O\left(\frac{\gamma_I^2}{\omega_{*i}}\right), \tag{38}$$

Thus, at this resonant value of $n_\varphi$ there is no FLR stabilization, i.e. whenever $\Delta'_B < 0$ there exists an unstable mode whose growth rate is actually enhanced, for small $\gamma_I/\omega_{*i}$, by a factor $2q/\sqrt{3}$ above the value it would have in the absence of diamagnetic effects.

## 5. Drift Resistive Ballooning Modes.

In this section we shall consider an ideal-MHD stable equilibrium, i.e. $\Delta'_B > 0$, and investigate drift resistive modes in the inviscid limit. Setting $\mu = 0$, Eq.(27) becomes

$$s^2 \frac{d}{dX}\left(\frac{X^2}{1+X^2}\frac{dU_0}{dX}\right) - Q_0 X^2 U_0 = 0, \tag{39}$$

with

$$Q_0 \equiv Q(\mu=0) = i\hat{\omega}(\hat{\omega}-\hat{\omega}_{*i})(\hat{\omega}-\hat{\omega}_{*e})\Big[1+2q^2P_0\Big] - \frac{\alpha^2}{2}\Big[1-P_0\Big], \tag{40}$$

and $P_0$ given by Eq.(32). Equation (39), subject to the boundary conditions

$$U_0(X \to \infty) = 0 \tag{41}$$

and

$$U_0(X \to 0) = \frac{1}{\Delta'_B} + \left(\frac{i}{\hat{\omega}-\hat{\omega}_{*e}}\right)^{1/2}\frac{\epsilon_\eta}{X} \tag{42}$$

to match the solution (14) or (15) in the ideal-MHD region, has the form of the canonical resistive ballooning equation considered for instance in Ref.[18], only the expression of our coefficient $Q_0$ being different from the standard ones. The solution to this boundary problem (in terms of confluent hypergeometric functions) is therefore known, and we can write the general dispersion relation for drift-resistive ballooning modes:

$$\epsilon_\eta \Delta'_B = -\left(\frac{\hat{\omega}-\hat{\omega}_{*e}}{i}\right)^{1/2}\frac{Q_0^{1/4}}{8s^{1/2}}\frac{\Gamma[(Q_0^{1/2}/s-1)/4]}{\Gamma[(Q_0^{1/2}/s+5)/4]}, \tag{43}$$

These modes can be driven unstable by a positive $\Delta'_B$ or, for even negligible $\epsilon_\eta\Delta'_B$ but finite pressure gradient, by the $\alpha^2$ term in $Q_0$. Two limits of this dispersion relation are of interest. The first one is $\epsilon_\eta\Delta'_B \gg 1$, i.e. close to the ideal-MHD instability threshold, where it yields

$$Q_0 = s^2. \tag{44}$$

The second one is $\epsilon_\eta \Delta'_B \ll 1$, i.e. away from the ideal-MHD instability, where the dispersion relation reduces to

$$Q_0 = -\left[\frac{2\Gamma(5/4)}{\Gamma(3/4)}\right]^4 \frac{s^2(\epsilon_\eta \Delta'_B)^4}{(\hat{\omega} - \hat{\omega}_{*e})^2}. \tag{45}$$

The general expression (43) provides a continuous transition between these two limits.

The approximate dispersion relation $Q_0 = s^2$, valid in the vicinity of the ideal-MHD instability threshold where $\epsilon_\eta \Delta'_B \to \infty$, can be written as

$$\begin{aligned} i\omega(\omega - \omega_{*i})(\omega - \omega_{*e})\Big[(1+2q^2)\omega_s^2 - \omega(\omega - \omega_{*e})\Big] \; = \\ = \; \omega_\eta \omega_A^2 \Big[s^2 \omega_s^2 - (s^2 + \alpha^2/2)\, \omega(\omega - \omega_{*e})\Big]. \end{aligned} \tag{46}$$

Similar to the previous section discussion after Eq.(35), the left-hand side of Eq.(46) indicates now the presence of four waves: one ion and one electron drift waves plus the two toroidally modified electron drift-acoustic waves. The effect of the electron drift-acoustic waves is lost in both the $\omega_s \to \infty$ and $\omega_s \to 0$ limits. In the incompressible limit ($\omega_s \to \infty$) Eq.(46) reduces to a dispersion relation analogous to that found in the theory of internal kink modes near the ideal-MHD marginal point [11,23]:

$$i\omega(\omega - \omega_{*i})(\omega - \omega_{*e}) \; = \; \frac{\omega_\eta \omega_A^2 s^2}{1+2q^2}. \tag{47}$$

In the absence of diamagnetic effects this has the solution $\omega = i[\omega_\eta \omega_A^2 s^2/(1+2q^2)]^{1/3}$, which has two damped roots and one unstable root with a strong resistive growth rate proportional to $\omega_\eta^{1/3}\omega_A^{2/3}$. Finite $\omega_{*j}$ diamagnetic effects mitigate this resistive instability, yielding instead two damped modes with real frequencies in the vicinity of $\omega_{*i}$ and $\omega_{*e}$ respectively, and one unstable mode with real frequency close to 0 and a weak resistive growth rate proportional to $\omega_\eta \omega_A^2 \omega_{*i}^{-2}$. Analogous results hold in the limit $\omega_s \to 0$, substituting $s^2 + \alpha^2/2 > 0$ for $(1+2q^2)^{-1}$. The coupling to the electron drift-acoustic waves at finite $\omega_s$ introduces two new roots of Eq.(46), one of which develops a strong resistive growth rate when the resonance condition (37) is satisfied. At this point, the new drift-acoustic root with real frequency around $2\omega_{*e}$ is damped, but one of the two nearly degenerate roots with real frequencies around $\omega_{*i}$ has a strong resistive growth rate proportional to $\omega_\eta^{1/2}\omega_A|\omega_{*i}|^{-1/2}$.

Away from the ideal-MHD instability threshold, i.e. for the range of equilibrium parameters where $0 \le \Delta'_B \lesssim 1$, we have $\epsilon_\eta \Delta'_B \ll 1$ and the approximate dispersion relation (45) holds. This can be

written as

$$i\omega(\omega-\omega_{*i})(\omega-\omega_{*e})\Big[(1+2q^2)\omega_s^2-\omega(\omega-\omega_{*e})\Big] \;=$$
$$=\;-\left[\frac{2\Gamma(5/4)}{\Gamma(3/4)}\right]^4\frac{\omega_\eta^3\omega_A^2 s^2{\Delta'_B}^4}{(\omega-\omega_{*e})^2}\Big[\omega_s^2-\omega(\omega-\omega_{*e})\Big]\;-\;\frac{\alpha^2}{2}\,\omega_\eta\omega_A^2\omega(\omega-\omega_{*e}). \tag{48}$$

Similar to the previously discussed dispersion relations (35) and (46), the right-hand side of Eq.(48) contains the instability drive. Here the two different resistive ballooning driving mechanisms, namely the global ideal-MHD energy drive represented by the term proportional to ${\Delta'_B}^4$, and the local pressure gradient and geodesic curvature drive represented by the Carreras-Diamond term proportional to $\alpha^2$, are explicitly shown. In the absence of these driving terms, the left-hand side of (48) would yield the ion and electron drift waves and the pair of electron drift-acoustic waves. The effect of the electron drift-acoustic waves as well as the $\alpha^2$ drive are lost in the incompressible limit: taking $\omega_s \to \infty$, Eq.(48) reduces to

$$-i\omega(\omega-\omega_{*i})(\omega-\omega_{*e})^3 \;=\; \left[\frac{2\Gamma(5/4)}{\Gamma(3/4)}\right]^4\frac{\omega_\eta^3\omega_A^2 s^2{\Delta'_B}^4}{1+2q^2}. \tag{49}$$

This is the generalization, including finite diamagnetic drift frequencies, of the resistive ballooning mode dispersion relation derived in Refs.[11-13]. For vanishing $\omega_{*j}$, this predicts an instability whose growth rate follows the "tearing mode scaling", being proportional to ${\omega_\eta}^{3/5}{\omega_A}^{2/5}{\Delta'_B}^{4/5}$.

For plasma parameters of interest at the edge of high-performance H-mode tokamak discharges, the $\alpha^2$ drive is the dominant one. Thus, neglecting $\Delta'_B$, we get the simplified dispersion relation

$$-i(\omega-\omega_{*i})\Big[(1+2q^2)\omega_s^2-\omega(\omega-\omega_{*e})\Big] \;=\; \frac{\alpha^2}{2}\,\omega_\eta\omega_A^2, \tag{50}$$

or $Q_0 = 0$. This dispersion relation generalizes the results of Refs.[10,22] by including the effect of sound wave propagation and coupling to the electron drift-acoustic waves. If we neglect the sound wave propagation, i.e. setting $\omega_s = 0$ in Eq.(50), we recover the result of Ref.[22]:

$$i\omega(\omega-\omega_{*i})(\omega-\omega_{*e}) \;=\; \gamma_{CD}^3, \tag{51}$$

where $\gamma_{CD} = (\alpha^2/2)^{1/3}\omega_\eta^{1/3}\omega_A^{2/3}$ is the single-fluid Carreras-Diamond growth rate [10]. Like in the analysis of modes near the ideal-MHD instability threshold, we see, as noted in [22], that the diamagnetic drift terms mitigate the strong single fluid resistive instability leaving only a weak resistive

instability with near-zero real frequency $\omega \simeq i\alpha^2\omega_\eta\omega_A^2/(2\omega_{*i}^2)$. However, our complete dispersion relation (50) shows that the growth rate of this instability is strongly enhanced when the low-frequency branch of the drift-acoustic mode is degenerate with the ion drift wave according to the resonance condition (37). At this point, due to the previously discussed mechanism responsible for the loss of FLR stabilization of ideal modes, a strong resistive instability

$$\omega \simeq \omega_{*i} \pm (i-1)\frac{\alpha}{2\sqrt{3}}\left(\frac{\omega_\eta\omega_A^2}{|\omega_{*i}|}\right)^{1/2} \tag{52}$$

is again found. This resonant peak of the resistive growth rate is shown in Fig. 3, where $Im(\omega)$ is plotted versus $n_\varphi$, for the same plasma parameters used in Fig. 2, except that now $\alpha = 1.0 < \alpha_{crit}$; the magnetic Reynolds number is taken to be $S \equiv \omega_A r^2/\eta_\parallel = 1.25\ 10^5$ and $\Delta'_B$ is neglected. The dependence of the mode frequency on $n_\phi$ is shown in Fig.4, where the ion diamagnetic frequency $\omega_{*i}$ is also shown.

## 6. Visco-Resistive Ballooning Modes.

Perpendicular viscous effects enter Eq.(27) in two ways. The term $T$ contains the viscous drag on the perturbed perpendicular velocity and agrees with results in [23,24]. The factor $P$ contains the viscous drag on the parallel flow and introduces, as noted in [25], a strong toroidal enhancement of the viscosity in the limit $\omega_s \to \infty$. Assuming that the perpendicular viscosity is given by its classical value, we have $\hat{\mu} = 0.15\beta_e(m_i/m_e)^{1/2}$ and, typically, $\hat{\mu} \ll 1$. In this case we can linearize $P(\hat{\mu}; X^2) \simeq P_0 + \hat{\mu}P_1(X^2)$, and Eq.(27) becomes:

$$s^2\frac{d}{dX}\left(\frac{X^2}{1+X^2}\frac{dU_0}{dX}\right) - \left(Q_0X^2 + T_0X^4\right)U_0 = 0, \tag{53}$$

with $P_0$ and $Q_0$ given by Eqs.(32,40), and

$$T_0 = i\hat{\mu}(1+8q^2P_0^2)(\hat{\omega}-\hat{\omega}_{*i})(\hat{\omega}-\hat{\omega}_{*e})^2 + 2\hat{\mu}\alpha^2P_0^2\left[(\hat{\omega}-\hat{\omega}_{*e})/\hat{\omega}_s\right]^2. \tag{54}$$

Moreover, for $\epsilon_\eta\Delta'_B \ll 1$ i.e. away from the ideal-MHD instability threshold, the magnitude of both $Q_0$ and $T_0$ is much less than unity. Thus, restricting ourselves to this case, we can solve Eq.(53) in two asymptotic regions. First, an inner region $|X| \sim 1$, where it reduces to

$$s^2\frac{d}{dX}\left(\frac{X^2}{1+X^2}\frac{dU_0^I}{dX}\right) = 0, \tag{55}$$

and has the following solution satisfying the ideal-MHD matching condition:

$$U_0^I \;=\; \frac{1}{\Delta'_B} \;+\; \epsilon_\eta \left( \frac{i}{\hat{\omega} - \hat{\omega}_{*e}} \right)^{1/2} \left( \frac{1}{X} - X \right). \tag{56}$$

Then, an outer region $|X| \gg 1$, where it reduces to

$$s^2 \, \frac{d^2 U_0^{II}}{dX^2} \;-\; \left( Q_0 X^2 \;+\; T_0 X^4 \right) U_0^{II} \;=\; 0, \tag{57}$$

and whose solution is subject to the matching condition $U_0^{II}(X \to 0) = U_0^I(X \to \infty)$. Now we can obtain a variational form of the visco-resistive dispersion relation using the trial function

$$U_0^{II}(X) = X^{1/2} K_{1/4}(\sigma X^2) \left\{ \frac{1}{\Delta'_B} - \left[ \epsilon_\eta \left( \frac{i}{\hat{\omega} - \hat{\omega}_{*e}} \right)^{1/2} - \frac{(\sigma/2)^{1/2} \, \Gamma(3/4)}{\Delta'_B \, \Gamma(5/4)} \right] X \right\}, \tag{58}$$

where $K_{1/4}$ is the modified Bessel function and $\sigma$ is a variational parameter. This choice of trial function satisfies identically the matching condition to $U_0^I(X)$ besides the decay condition at infinity, and reproduces the exact eigenfunction in the inviscid limit $T_0 = 0$. For negligible $\Delta'_B$ drive, the resulting variational dispersion relation is

$$Q_0 + 2.46 (s T_0)^{2/3} = 0. \tag{59}$$

The numerical solution of this variational visco-resistive dispersion relation is displayed in Fig.5, for the same parameters used in Fig.3 and $\hat{\mu} = 0.003$. It shows that the viscosity reduces the growth rate of the drift resistive ballooning mode, especially at very large toroidal mode numbers, but it does not affect much the growth rate peak at the resonant value of $n_\varphi$.

## 7. Conclusions.

By making use of the $s - \alpha$ equilibrium description of a Tokamak, a simple differential eigenvalue equation describing linear resistive ballooning instabilities has been derived. This equation (Eq.(27)) is appropriate for collisional plasma conditions in the edge pedestal region of a Tokamak. This extends the original analyses [10,22] of resistive ballooning modes, by describing the effects of matching to the ideal region, of coupling to electron drift-acoustic modes, and of perpendicular viscosity. When $\alpha > \alpha_{crit}$ (the critical value for ideal-MHD, $n_\phi \to \infty$, ballooning instability) coupling to drift-acoustic

waves removes ion FLR stabilization of ideal-MHD modes at a particular range of wavelength, i.e. a particular toroidal mode number. In addition, when $\alpha < \alpha_{crit}$ and ideal modes are no longer unstable, the same coupling mechanism causes the growth rate of drift-resistive ballooning modes (drift-RBM) to peak in this range of wavelengths. In practice, however, for parameters typical of the edge pedestal in Alcator C-Mod, ($\omega_s/\omega_A \sim 0.02$, $\omega_{*i}/n_\phi\omega_A \sim 0.05$, $q = 5$) these effects are predicted to appear at very low values of $n_\phi = 2$ or 3. In the absence of ion viscous damping a broad spectrum of unstable drift-RBMs is predicted to be unstable so that the transition between ELM-free H-mode and the EDA-mode in Alcator C-Mod (in which a single Quasi Coherent Eigenmode with $n_\phi \sim 20$ appears in the pedestal region) cannot be explained within the context of linear drift-RBM theory.

Addition of perpendicular ion viscous effects has been studied in a variational formalism. This indicates that the unstable spectrum of RBMs may be truncated by viscosity, with shorter wavelength modes being stabilized as $\mu$ is increased. But viscous effects cannot expain the appearance of a relatively short wavength ($n_\phi \sim 20$) mode before other wavelengths, as the H-mode pedestal steepens.

The foregoing drift-RBM analysis might be considered to be relevant to the, so called, "washboard modes" [26] which have been observed in the edge of JET plasmas as the H-mode pedestal re-establishes itself following its collapse in a Type I ELM event. "Washboard modes" have toroidal mode numbers in the range $1 \leq n_\phi \leq 10$ and may therefore coincide with the truncated spectrum (see Fig.5) predicted when ion perpendicular viscosity is added to the drift-RBM analysis. However, they are reported to propagate in the direction of the electron diamagnetic drift, whereas, as shown in Fig.4, the drift-RBMs of the present analysis are ion modes.

**Acknowledgements.**

We thank Peter Catto for very helpful discussions and encouragement. This work was supported by the U.S. Department of Energy grant No. DE-FG02-91ER-54109 at M.I.T.

## References


[1] A.E. Hubbard et al., Phys. Plasmas **8**, 2033 (2001).

[2] S.V. Novakovskii, P.N. Guzdar, J.F. Drake, C.S. Liu and F.L. Waelbroeck, Phys. Plasmas **2**, 781 (1995).

[3] J.R. Myra, D.A. D'Ippolito, X.Q. Xu and R.H. Cohen, Phys. Plasmas **7**, 4622 (2000).

[4] B.N.Rogers and J.F.Drake Phys. Plasmas **6**, 2797 (1999).

[5] X.Q. Xu, R.H. Cohen, T.D. Rognlien and J.R. Myra, Phys. Plasmas **7**, 1951 (2000).

[6] B.N. Rogers and J.F. Drake, Phys. Rev. Letts. **79**, 229 (1997).

[7] S.I. Braginskii, in Reviews of Plasma Physics, edited by M.A. Leontovich (Consultants Bureau, New York, 1965), Vol.I, p.205.

[8] D.A. Mossessian et al., Plasma Phys. Controlled Fusion **44**, 423 (2002).

[9] J.W.Connor, R.J.Hastie and J.B.Taylor Phys. Rev. Lett. **40**, 396 (1978).

[10] B. Carreras, P. Diamond, M. Murakami, et al. Phys. Rev. Lett. **50**, 503 (1983).

[11] H.R. Strauss, Phys. Fluids **24**, 2004 (1981).

[12] J.W. Connor et al. Plasma Physics and Controlled Fusion Research, Proc. 9th IAEA Conf. (IAEA, Vienna. 1983) Vol.III,p.403.

[13] J.F. Drake and T.M. Antonsen, Phys. Fluids **28**, 544 (1985).

[14] J.W. Connor and R.J. Hastie, Plasma Phys. Controlled Fusion **27**, 621 (1985).

[15] A. Zeiler, J.F. Drake and B. Rogers, Phys. Plasmas **4**, 2134 (1997).

[16] W.M. Tang, R.L. Dewar and J. Manickam, Nucl. Fusion **22**, 1079 (1982).

[17] R.J. Hastie, P.J. Catto and J.J. Ramos Phys. Plasmas **7**, 4561 (2000).

[18] D. Correa-Restrepo, Z. Naturforsch. **37a**, 848 (1982).

[19] A.H. Glasser, J.M. Greene and J.L. Johnson, Phys. Fluids **18** 875 (1975).

[20] O.P. Pogutse and E.I. Yurchenko, in Reviews of Plasma Physics, edited by M.A. Leontovich (Consultants Bureau, New York, 1965), Vol.11, p65

[21] T. Hender, K. Grassie and H. Zehrfeld, Nucl. Fus. **29**, 1459 (1989).

[22] P.H. Diamond, P.L. Similon, T.C. Hender and B.A. Carreras, Phys. Fluids **28**, 1116 (1985).

[23] G. Ara, B. Basu and B. Coppi, Phys. Fluids **22**, 672 (1979).

[24] B. Coppi and F. Porcelli, Phys. Rev. Lett. **57**, 2272 (1986).

[25] V.P. Lakhin and A.B. Mikhailovskii Phys. Lett. A **191**, 162 (1994).

[26] P.Smeulders et al., Plasma Phys. Contrl. Fusion, **41**, 1303 (1999).

**Figure Captions.**

Fig.1 FLR-modified growth rate of ideal ballooning modes as a function of toroidal mode number, $n_\phi$. Plasma parameters are: $s = 2,\ q = 5,\ \omega_{*i}/n_\phi\omega_A = -\omega_{*e}/n_\phi\omega_A = 0.02,\ \Delta'_B = -50$ (corresponding to $\alpha = 1.185 = 1.01\alpha_{crit}$). The $O(1/n)$ correction to the ideal-MHD quantity, $\Delta'_B$ has been neglected. The solid curve is for $\omega_s/\omega_A = 0$ and the dashed curve is for the incompressible limit, $\omega_s/\omega_A \to \infty$.

Fig.2 FLR-modified ideal ballooning growth rate, versus $n_\phi$ for $\omega_s/\omega_A = 0.05$. Other parameters are as in Fig.1.

Fig.3 Growth rate of the drift-resistive ballooning mode (from Eq.(50)) against toroidal mode number, $n_\phi$. Parameters are: $s = 2,\ q = 5,\ \omega_{*i}/n_\phi\omega_A = -\omega_{*e}/n_\phi\omega_A = 0.02,\ \alpha = 1.0,\ S = 1.25\ 10^5$.

Fig.4 Frequency of the Drift RBM against toroidal mode number, $n_\phi$. The linear dependence of the ion diamagnetic frequency, $\omega_{*i}$, is also shown by the dashed line.

Fig.5 Effect of perpendicular ion viscosity on the drift-resistive ballooning mode growth rate. Solid curve is for $\hat{\mu} = 0.003$, dashed curve is for $\hat{\mu} = 0$ (as in Fig.3). Other parameters are as in Fig.3.

Fig.1

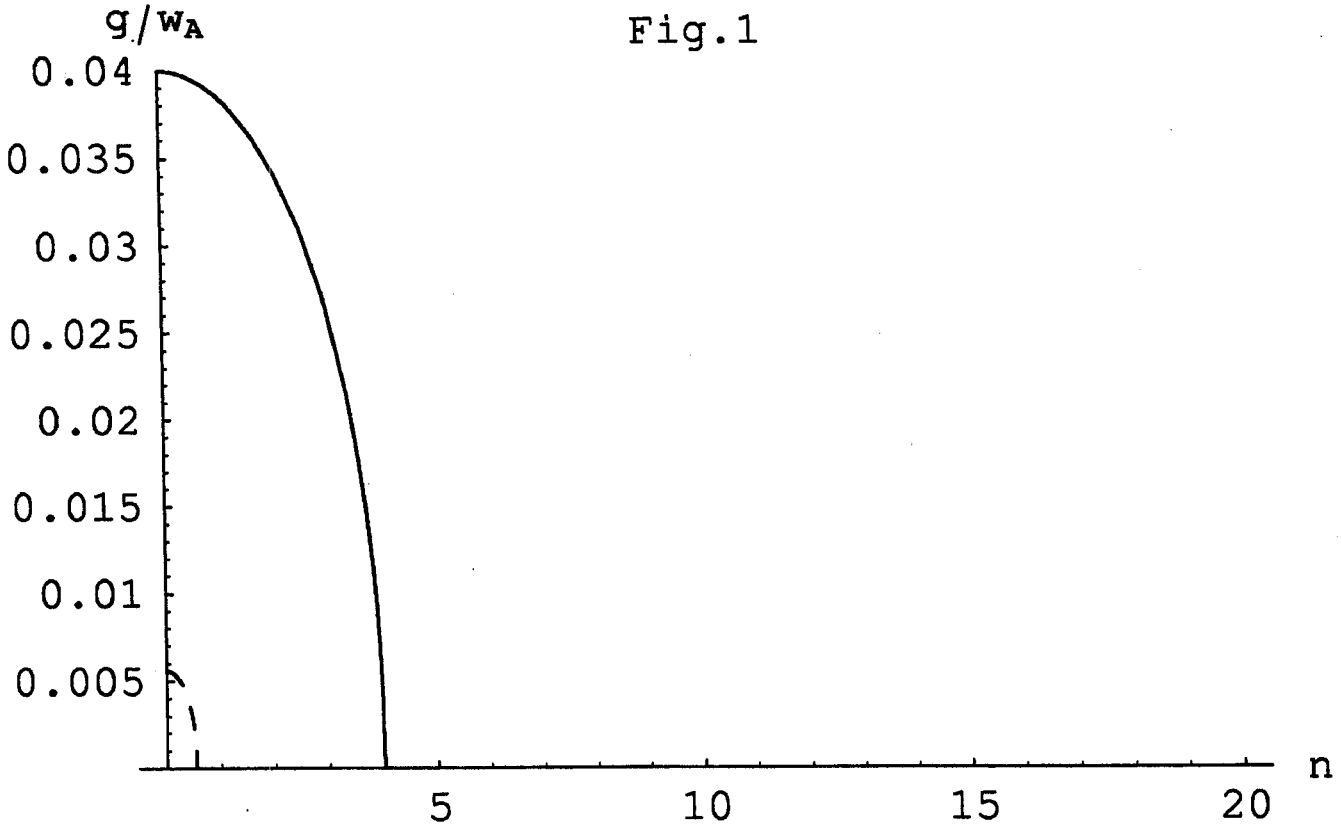

Fig.2

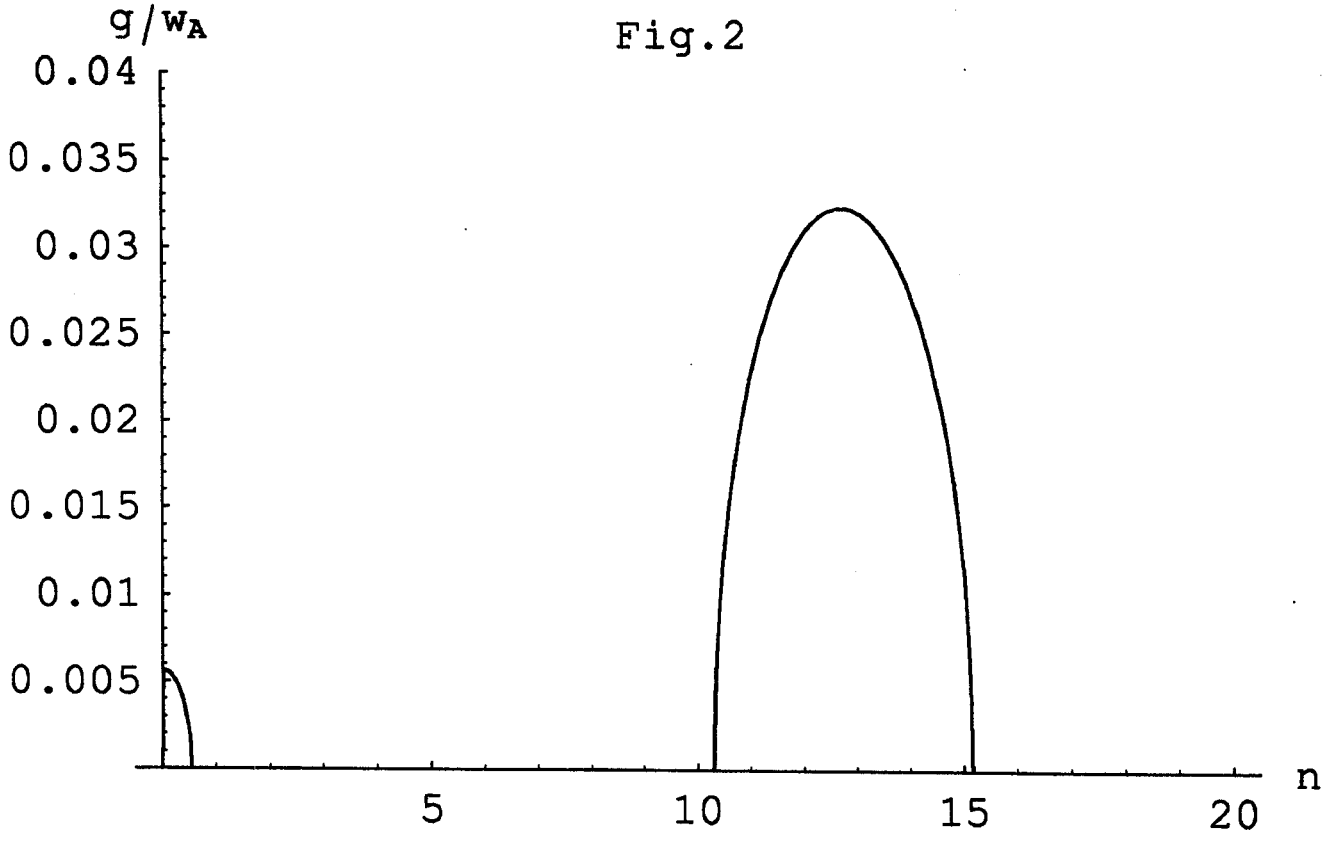

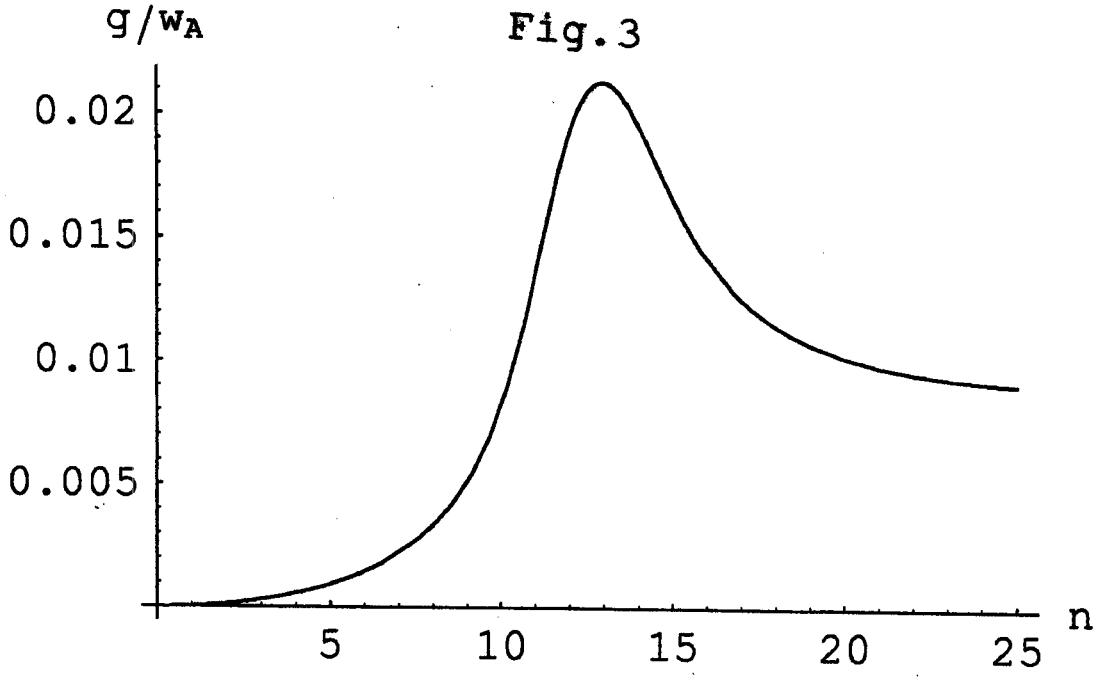


Fig.3

Fig. 4

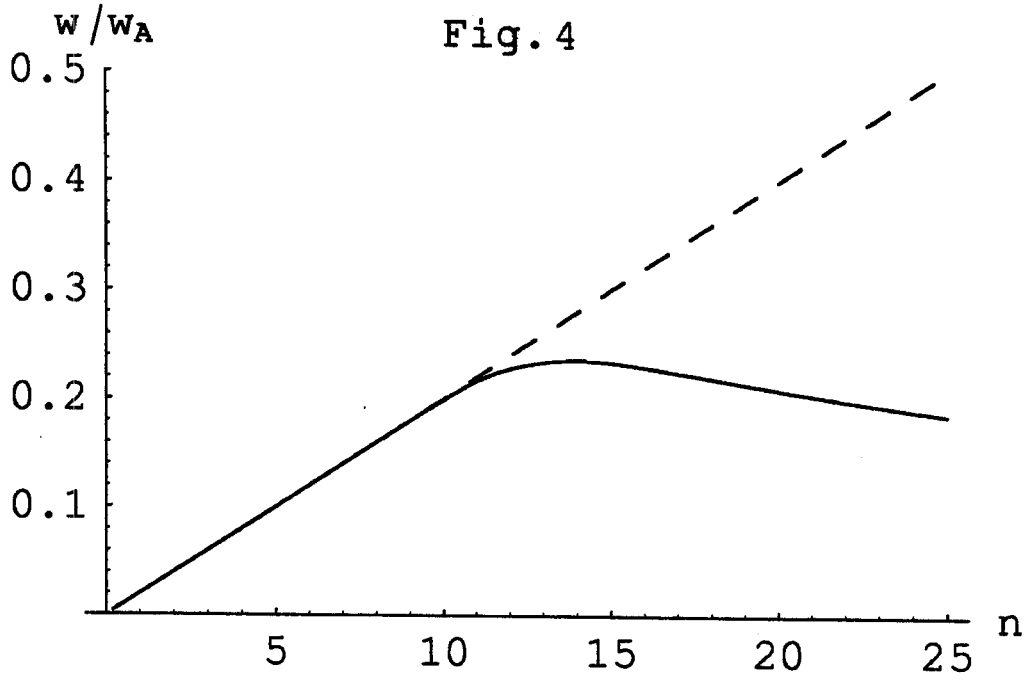

Fig.5